

Mechanical Activation of Catalysts for C–C Bond Forming and Anionic Polymerization Reactions from a Single Macromolecular Reagent

Andrew G. Tennyson, Kelly M. Wiggins, and Christopher W. Bielawski*

Department of Chemistry and Biochemistry, The University of Texas at Austin, Austin, Texas 78712, United States

Received August 23, 2010; E-mail: bielawski@cm.utexas.edu

Abstract: Coupling of pyridine-capped poly(methyl acrylate)s, PyP_M (where M corresponds to the number average molecular weight in kDa), to the SCS-cyclometalated dipalladium complex $[(1)(\text{CH}_3\text{CN})_2]$ afforded organometallic polymers $[(1)(\text{PyP}_M)_2]$ with a concomitant doubling in molecular weight. Ultrasonication of solutions containing $[(1)(\text{PyP}_M)_2]$ effected the mechanical scission of a palladium–pyridine bond, where the liberated PyP_M was trapped with excess HBF_4 as the corresponding pyridinium salt, harnessed to effect the stoichiometric deprotonation of a colorimetric indicator, or used to catalyze the anionic polymerization of α -trifluoromethyl-2,2,2-trifluoroethyl acrylate. The mechanically induced chain scission also unmasked a catalytically active palladium species which was used to facilitate carbon–carbon bond formation between benzyl cyanide and *N*-tosyl imines. Spectroscopic and macromolecular analyses as well as a series of control experiments demonstrated that the aforementioned structural changes were derived from mechanical forces that originated from ultrasound-induced dissociation of the polymer chains connected to the aforementioned Pd complexes.

Introduction

Ultrasonication has recently received significant attention for its ability to alter the chemical structures, properties, and functions of polymeric materials via mechanical force, a process termed “mechanochemistry”.^{1,2} During the application of ultrasonic energy to a solution of polymers, bubbles are created and rapidly collapse which induces velocity gradients and attendant stresses to the solvated polymer chains.³ For macromolecules of sufficient chain length, this mechanical force may effect chain scission⁴ or isomerization⁵ at centrally located sites.¹ Because mechanochemistry ultimately enables access to thermally inaccessible pathways,^{4,5} there has been substantial interest in developing mechanically activated catalysts. For example,

recent efforts by Sijbesma have highlighted the promise for using sonochemically induced changes in polymer structure to drive catalytic olefin metathesis and transesterification reactions.⁶ More broadly, mechanocatalysts^{4b} are anticipated to uncover fundamentally new chemistries, enable transformations not currently feasible,⁷ and endow stimulus-responsive materials with novel functions and applications.⁸ Achieving many of these goals, however, hinges on using mechanical force to access new reaction pathways, particularly those that are thermally inaccessible or prohibited.

To guide the design of such mechanically activated catalysts, we first considered the components necessary for a mechano-responsive material:¹ (i) a mechanophore,^{1,4,5} which undergoes an electronic or structural change in response to mechanical force and (ii) an actuator, which translates exogenously supplied energy into useful mechanical force at the mechanophore.⁹ Polymers have been extensively employed as actuators, given that they respond to mechanical stress at both the macro- and microscopic level and can be covalently linked to small

- (1) Caruso, M. M.; Davis, D. A.; Shen, Q.; Odom, S. A.; Sottos, N. R.; White, S. R.; Moore, J. S. *Chem. Rev.* **2009**, *109*, 5755.
- (2) Mason, T. J.; Lorimer, J. P. *Applied Sonochemistry*; Wiley-VCH: New York, 2002.
- (3) Basedow, A. M.; Ebert, K. H. *Adv. Polym. Sci.* **1977**, *22*, 83.
- (4) (a) Berkowski, K. L.; Potisek, S. L.; Hickenboth, C. R.; Moore, J. S. *Macromolecules* **2005**, *38*, 8975. (b) Karthikeyan, S.; Potisek, S. L.; Piermattei, A.; Sijbesma, R. P. *J. Am. Chem. Soc.* **2008**, *130*, 14968. (c) Kryger, M. J.; Ong, M. T.; Odom, S. A.; Sottos, N. R.; White, S. R.; Martinez, T. J.; Moore, J. S. *J. Am. Chem. Soc.* **2010**, *132*, 4558.
- (5) (a) Hickenboth, C. R.; Moore, J. S.; White, S. R.; Sottos, N. R.; Baudry, J.; Wilson, S. R. *Nature* **2007**, *446*, 423. (b) Potisek, S. L.; Davis, D. A.; Sottos, N. R.; White, S. R.; Moore, J. S. *J. Am. Chem. Soc.* **2007**, *129*, 13808. (c) Davis, D. A.; Hamilton, A.; Yang, J.; Cremar, L. D.; Van Gough, D.; Potisek, S. L.; Ong, M. T.; Braun, P. V.; Martinez, T. J.; White, S. R.; Moore, J. S.; Sottos, N. R. *Nature* **2009**, *459*, 68. (d) Lenhardt, J. M.; Black, A. L.; Craig, S. L. *J. Am. Chem. Soc.* **2009**, *131*, 10818. (e) Wiggins, K. M.; Hudnall, T. W.; Shen, Q.; Kryger, M. J.; Moore, J. S.; Bielawski, C. W. *J. Am. Chem. Soc.* **2010**, *132*, 3256. (f) Lenhardt, J. M.; Ong, M. T.; Choe, R.; Evenhuis, C. R.; Martinez, T. J.; Craig, S. L. *Science* **2010**, *329*, 1057.

- (6) Piermattei, A.; Karthikeyan, S.; Sijbesma, R. P. *Nature Chem.* **2009**, *1*, 133.
- (7) (a) Anastas, P. T.; Kirchhoff, M. M.; Williamson, T. C. *Appl. Catal., A* **2008**, *221*, 3. (b) Madhavan, N.; Jones, C. W.; Weck, M. *Acc. Chem. Res.* **2008**, *41*, 1153.
- (8) (a) White, S. R.; Sottos, N. R.; Geubelle, P. H.; Moore, J. S.; Kessler, M. R.; Sriram, S. R.; Brown, E. M.; Viswanathan, S. *Nature* **2001**, *409*, 794. (b) Xiangxu, C.; Dam, M. A.; Ono, K.; Mal, A.; Shen, H.; Nutt, S. R.; Sheran, S. R.; Wudl, F. *Science* **2002**, *295*, 1698. (c) White, S. R.; Caruso, M. M.; Moore, J. S. *MRS Bull.* **2008**, *33*, 766. (f) Wool, R. P. *Soft Mater.* **2008**, *4*, 400. (d) Williams, K. A.; Dreyer, D. R.; Bielawski, C. W. *MRS Bull.* **2008**, *33*, 759. (e) Kolmakov, G. V.; Matyjaszewski, K.; Balazs, A. C. *ACS Nano* **2009**, *3*, 885.
- (9) Luche, J. L.; Einhorn, J.; Einhorn, J. J.; Sinisterra-Gago, J. V. *Tetrahedron Lett.* **1990**, *31*, 4125.

molecules.¹ Conductive polymer-based actuators are those that are viscoelastic and can be obtained by synthetic methods which enable accurate prediction and control of molecular weight.¹ Poly(methyl acrylate) (PMA), in particular, exhibits the desired macromolecular and mechanical properties and can be prepared in a wide range of predetermined molecular weights using the SET-LRP method developed by Percec.^{10,11} Moreover, actuators comprising PMA chains have been successfully utilized by Moore,^{4c,5a–c} and more recently by us,^{5e} to exert force upon mechanophores and to induce structural as well as functional changes therein. Finally, because a complete catalytic cycle necessitates both substrate binding and product release, a catalyst generated in response to ultrasonically induced mechanical force must retain this critical function.

Guided by these considerations, we concluded that a transition metal complex, when coordinated to an actuating ligand, would serve as an ideal mechanophore for achieving mechanically activated catalytic functions. Pioneering studies by Weck¹² and Craig¹³ have demonstrated that certain SCS-, NCN-, and PCP-cyclometalated palladium(II) complexes exhibit reversible metal–pyridine interactions, even when both components are appended with polymer chains. Moreover, these organometallic systems have been shown to participate in the catalytic formation of carbon–carbon bonds (e.g., Heck-type coupling), albeit under thermal control. Inspired by these results, we reasoned that a macromolecular complex, comprising a palladium(II) center ligated by a pyridine–PMA conjugate, should exhibit sonochemically induced structural dynamism that would be accompanied by activation of metal- as well as base-mediated catalytic reactions in response to applied mechanical force. Herein we demonstrate the viability of such a mechanophore–actuator construct to function as a mechanocatalyst, whereby ultrasonication liberates two catalytically active functionalities that effect two orthogonal chemical reactivities: Pd-catalyzed C–C coupling and base-catalyzed, anionic polymerization reactions. To the best of our knowledge, our findings represent the first demonstration of the activation of such catalytic reactions in response to mechanical force and establish a foundation for achieving the aforementioned goals.

Results and Discussion

To access the desired mechanoresponsive reagent, we first synthesized the requisite pyridine-capped PMA-based actuators (**PyP_M**, Figure 1) of varying molecular weights (where M corresponds to the number average molecular weight (M_n) in kDa of the PMA chain **P_M**; see Table 1) via SET-LRP of methyl acrylate¹⁰ using 4-pyridinyl-2-bromoisobutyrate as the initiator. In parallel, the SCS-cyclometalated dipalladium(II) salt [(**1**)(CH₃CN)₂] was selected as a complementary mechanophore and was prepared using established methods.¹⁴ Combining **PyP_M**

with 0.5 equiv of [(**1**)(CH₃CN)₂] in DMF at room temperature for 16 h resulted in a doubling of M_n , as determined by gel permeation chromatography (GPC), that was consistent with the facile displacement of CH₃CN by pyridine-based ligands to afford [(**1**)(**PyP_M**)₂] (step i, Figure 1; results summarized in Table 1). Similarly, treatment of [(**2**)(CH₃CN)] with **PyP₁₁₀** produced the end-capped derivative [(**2**)(**PyP₁₁₀**)]. Additional support for the binding of **PyP_M** to Pd in [(**1**)(**PyP_M**)₂] and [(**2**)(**PyP₁₁₀**)] was obtained via ¹H NMR spectroscopic analysis, wherein the signals for the 2,6-protons in the pyridyl moieties shifted upfield from 8.57 ppm (CDCl₃) in free **PyP_M** to 8.23 ppm in the Pd complexes, reflecting their proximity to arene ring currents upon coordination (see Figures S1–S3, Supporting Information).

Because the mechanophore in [(**1**)(**PyP_M**)₂] occupies the center of the polymer chain, sonication of solutions thereof was anticipated to afford [(**1**)(**PyP_M**)(CH₃CN)] and **PyP_M** via Pd–pyridine bond scission (step ii, Figure 1).¹⁵ Upon cessation of the sonication, however, these species were found to recombine in solution with no net effect on M_n (step iii, cf. Figure S7, Supporting Information). Therefore, we selected HBF₄ to trap any liberated **PyP_M** as its corresponding pyridinium tetrafluoroborate salt [**HPyP_M**][BF₄] (step iv). Sonication of CH₃CN solutions containing [(**1**)(**PyP_M**)₂] (where M = 21, 25, and 66) and excess HBF₄ in a Suslick¹⁶ cell at 4 °C for 2 h afforded a halving of the polymer's M_n (see Figure 2A for M = 66), consistent with the anticipated cleavage of a single Pd–N bond. Control experiments performed in the absence of sonication (at both 4 and 25 °C) revealed that the polymers analyzed displayed unaltered M_n values, indicating that the HBF₄ did not cause chain scission via protonation of the coordinated pyridine moieties. Likewise, no change in the M_n was observed for the [(**1**)(**PyP_M**)₂] containing shorter chains (M = 7 and 11), consistent with the minimum chain-length threshold requirement for a polymer to experience sonication-induced tensile force. The M_n value measured for [(**2**)(**PyP₁₁₀**)] was also unaffected by sonication, suggesting that the location of the scissile bond at the end of a polymer chain precluded application of vectorially opposed mechanomotive force on the Pd–pyridine bond.

To study the kinetics of the chain scission process, the decrease in the GPC refractive index (RI) signal attributed to [(**1**)(**PyP_M**)₂] was monitored by withdrawing aliquots from the reaction vessel at timed intervals during a typical sonication experiment.¹⁵ Analysis of the aliquots from the sonication of [(**1**)(**PyP₆₆**)₂] revealed a gradual decrease in M_n from 120 to 60 kDa that reached completion within 2 h (Figure 2B). Plotting $-\ln(I/I_0)$ vs time, where I_0 and I correspond to the RI signal for [(**1**)(**PyP₆₆**)₂] before sonication and at each time-point, respectively, enabled determination of the first-order rate of $3.6 \times 10^{-2} \text{ min}^{-1}$ (black line, Figure 2C). Both [(**1**)(**PyP₂₁**)₂] and [(**1**)(**PyP₂₅**)₂] exhibited slower rates (1.0 and $1.5 \times 10^{-2} \text{ min}^{-1}$, respectively), reflecting the decreased efficiency of cavitation-induced scission for these shorter-chain polymers (blue and red lines, respectively, Figure 2D). Consistent with the aforementioned bulk GPC analyses, neither [(**1**)(**PyP₇**)₂] nor [(**1**)(**PyP₁₁**)₂]

(10) Percec, V.; Guliashvili, T.; Ladislav, J. S.; Wistrand, A.; Stjernedahl, A.; Sienkowska, M. J.; Monteiro, M. J.; Sahoo, S. *J. Am. Chem. Soc.* **2006**, *128*, 14156.

(11) For examples of ultrasound-induced chain scission in poly(tetrahydrofuran)s containing coordinative Pd–P and Pt–P bonds, see: (a) Paulusse, J. M. J.; Sibjesma, R. P. *Angew. Chem., Int. Ed.* **2004**, *43*, 4459. (b) Paulusse, J. M. J.; Huijbers, J. P. J.; Sibjesma, R. P. *Chem.–Eur. J.* **2006**, *12*, 4928. (c) Paulusse, J. M. J.; Sibjesma, R. P. *Chem. Commun.* **2008**, *37*, 4416.

(12) (a) South, C. R.; Burd, C.; Weck, M. *Acc. Chem. Res.* **2007**, *40*, 63. (b) Yang, S. K.; Ambade, A. V.; Weck, M. *Chem.–Eur. J.* **2009**, *15*, 6605.

(13) (a) Loveless, D. M.; Jeon, S. L.; Craig, S. L. *J. Mater. Chem.* **2007**, *17*, 56. (b) Xu, D.; Craig, S. L. *J. Phys. Chem. Lett.* **2010**, *1*, 1683.

(14) Loeb, S. J.; Shimizu, G. K. H. *Chem. Commun.* **1999**, 1395.

(15) General sonication conditions: pulsed ultrasound (1.0 s on, 1.0 s off) was supplied at 23% power (10.1 W cm^{-2}) for 2 h. All sonications were performed on solutions with a final volume of 10 mL in a Suslick cell under a positive pressure of argon. The external temperature was maintained at 4 °C aided by the use of a cold room and ice-water bath. The internal temperatures of the sonicated solutions were monitored via a thermocouple and found to be ≤ 9 °C.

(16) Suslick, K. S.; Goodale, J. W.; Schubert, P. F.; Wang, H. H. *J. Am. Chem. Soc.* **1983**, *105*, 5781.

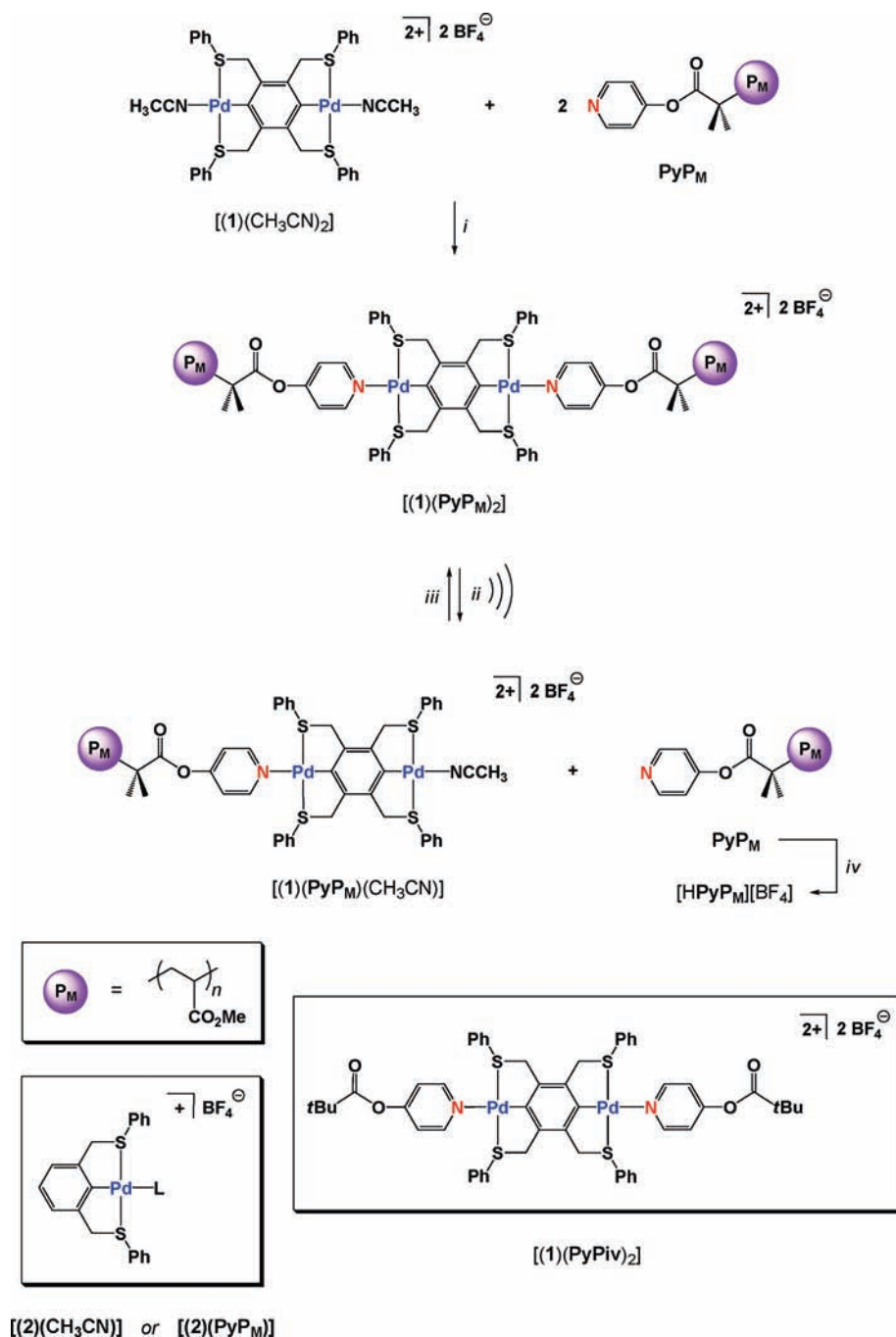


Figure 1. Synthesis and chain scission of mechanoresponsive Pd-based polymers. Conditions: (i) DMF, room temperature, 16 h; (ii) sonication for 2 h at 4 °C of $[(1)(PyP_M)_2]$ (10 mg) in CH_3CN (10 mL), and (iii) recoordination of PyP_M or (iv) trapping as $[HPyP_M][BF_4]$ with 20 equiv of HBF_4 .

Table 1. Summary of Molecular Weight Data for Chain Coupling and Scission Experiments^a

	PyP_M		$[(1)(PyP_M)_2]$			
			pre-sonication		post-sonication	
	M_n [kDa]	PDI	M_n [kDa]	PDI	M_n [kDa]	PDI
P₇	6.8	1.2	12	1.1	12	1.1
P₁₁	11	1.2	22	1.2	23	1.2
P₂₁	21	1.2	41	1.1	20	1.3
P₂₅	25	1.4	48	1.3	27	1.4
P₆₆	66	1.4	120	1.4	60	1.4

^a Number average and weight average molecular weights (M_n and M_w , respectively) were determined by GPC (eluent = DMF, 0.1 M LiBr) and are reported relative to polystyrene standards. Polydispersity indices (PDIs) were calculated using the equation $PDI = M_w/M_n$.

exhibited any change in RI signal (overlapping purple and orange lines, respectively; Figure 2D). Collectively, these results indicate that (i) a minimum chain length of approximately 40 kDa was required for chain scission to occur and (ii) increasing chain length beyond this threshold correlated with an increased rate of chain scission.

We sought to gain greater insight into the chemical process underlying the observed chain scission by employing a base-sensitive dye that would display a colorimetric response upon exposure to free pyridine. To perform this task, 4-[(4-anilino-phenyl)azo]benzenesulfonic acid (**3**) was selected given its

(17) Kolthoff, I. M.; Chantooni, M. K., Jr.; Bhowmik, S. *Anal. Chem.* **1967**, 39, 315.

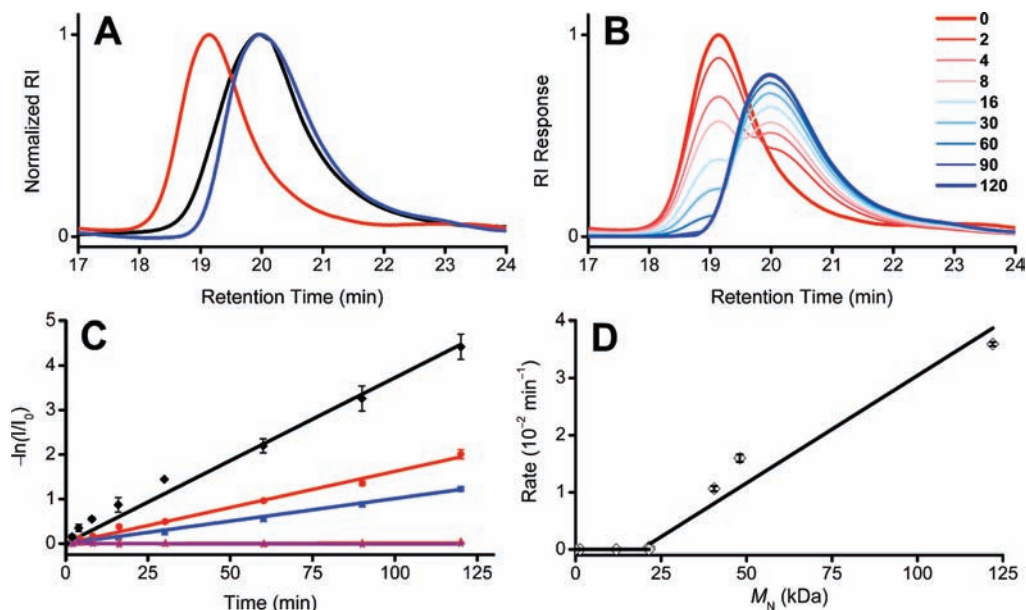


Figure 2. Representative examples of GPC traces and kinetic plots for the mechanochemical scission of [(1)(PyP_M)₂]. (A) GPC traces of [(1)(PyP₆₆)₂] before and after sonication (red and blue, respectively) overlaid with PyP₆₆ for comparison (black). (B) GPC data were acquired at timed intervals by analyzing aliquots removed during the sonication of [(1)(PyP₆₆)₂] ($t = 0$, topmost red); the gradual decrease in the peak intensity measured at retention time = 19.13 min ($t = 2$ –8 min, fading red) was accompanied by the appearance of a new peak measured at retention time = 19.89 min that was complete after 2 h ($t = 16$ –120 min, darkening blue). All aliquots analyzed consisted of an initial polymer concentration of 4 mg mL⁻¹. (C) First-order rate plot for the sonication of [(1)(PyP_M)₂], where $M = 66$ (black), 25 (red), 21 (blue), 11 (orange), and 7 (purple). I_0 and I correspond to the RI signal prior to sonication and at each time-point t thereafter, respectively. The RI intensity for each polymer was taken at the peak retention times (see Table S2, Supporting Information). (D) Plot of rate coefficients determined in C as a function of M_n . All data points and error bars were calculated from the average and standard deviation, respectively, of three separate experiments.

demonstrated viability¹⁷ for pH indication in CH₃CN and the detection of organic nitrogen bases.¹⁸ In CH₃CN solution, protonation of **3** by stoichiometric HBF₄ afforded [3H][BF₄] which exhibited a deep purple color. Gratifyingly, subsequent titration with 1 equiv of pyridine caused an immediate color change to yellow, consistent with the reformation of **3** (Figure 3A), and indicated that the system would be viable for detecting free PyP_M generated under sonication. Thus, we envisioned that a solution containing [(1)(PyP_M)₂] and [3H][BF₄] would undergo a similar color change upon sonication, reflecting the release of PyP_M upon cleavage of the Pd–pyridine bond.

In a typical experiment for the colorimetric detection of free PyP_M, a purple solution containing 10 μM [(1)(PyP_M)₂] and 10 μM [3H][BF₄] in 10 mL of CH₃CN was prepared and transferred to a Suslick cell, whereupon chain scission was induced using the aforementioned sonication conditions.¹⁵ Sonication of these polymers in the presence of [3H][BF₄] afforded a clear, yellow solution, consistent with its deprotonation by free PyP_M, and in good agreement with the reductions in polymer molecular weight observed by GPC for [(1)(PyP_M)₂] ($M = 21, 25,$ and 66) (Figure 3B). Subsequent addition of 1 equiv of HBF₄ restored the solution to its original purple color, evidence that sonication did not degrade the dye and generated 1 equiv of base. Because no changes in the optical or GPC profiles were noted in the absence of sonication, we concluded that thermally induced or proton-facilitated ligand displacement did not occur. As negative control experiments, the aforementioned indicator experiments were performed via sonication of (i) “sub-threshold” [(1)(PyP₇)₂] and [(1)(PyP₁₁)₂] (variants

shorter than the critical threshold needed to experience sonochemical tensile force) to confirm that mechanical activation derived from cavitation (for $M = 11$, see Figure 3C); (ii) end-capped [(2)(PyP₁₁₀)], to demonstrate that an internally located mechanophore was necessary for Pd–pyridine bond cleavage to occur (Figure 3D); and (iii) mechanophore model complex [(1)(PyPiv)₂] (see Figure 1) in the presence of 90 kDa PMA, to test whether the released base occurs only when the mechanophore was covalently linked to PMA actuators (Figure 3E). No color change was observed during any of these control experiments. Collectively, these results confirm that chain scission in [(1)(PyP_M)₂] occurred at the Pd–pyridine bond to liberate free PyP_M and was only effected when the criteria for delivery of ultrasonically induced mechanical force were satisfied.

Considering that the sonication of [(1)(PyP_M)₂] generated [(1)(PyP_M)(CH₃CN)] and PyP_M in situ, we envisioned exploiting these species for use in both metal- and base-catalyzed reactions. Elegant studies by Weck and Jones have shown that polymer- and silica-supported derivatives of [(2)(CH₃CN)] are capable of facilitating Heck-type coupling chemistry, albeit at 120 °C in DMF, and only upon reductive generation and release of zerovalent Pd.¹⁹ Given the success of these SCS-cyclopalladated systems at catalyzing carbon–carbon bond formation reactions, we envisioned that [(1)(PyP_M)₂] could catalyze a comparably illustrative coupling reaction under sonochemical conditions (i.e., nonthermal, in dilute solutions below 10 °C), optimally without disrupting the Pd oxidation state or coordination sphere. An ideal coupling reaction was recently described by Szabó, wherein [(2)(CH₃CN)] was found to catalyze carbon–carbon bond

(18) (a) Pudipeddi, M.; Zannou, E. A.; Vasanthavada, M.; Dontabhaktuni, A.; Royce, A. E.; Joshim, Y. M.; Serajuddin, A. T. M. *J. Pharm. Sci.* **2008**, *97*, 1831. (b) Karam, H.; El Kousy, N.; Towakkol, M. *Anal. Lett.* **1999**, *32*, 79.

(19) Yu, K.; Sommer, W.; Richardson, J. M.; Weck, M.; Jones, C. W. *Adv. Synth. Catal.* **2005**, *347*, 161.

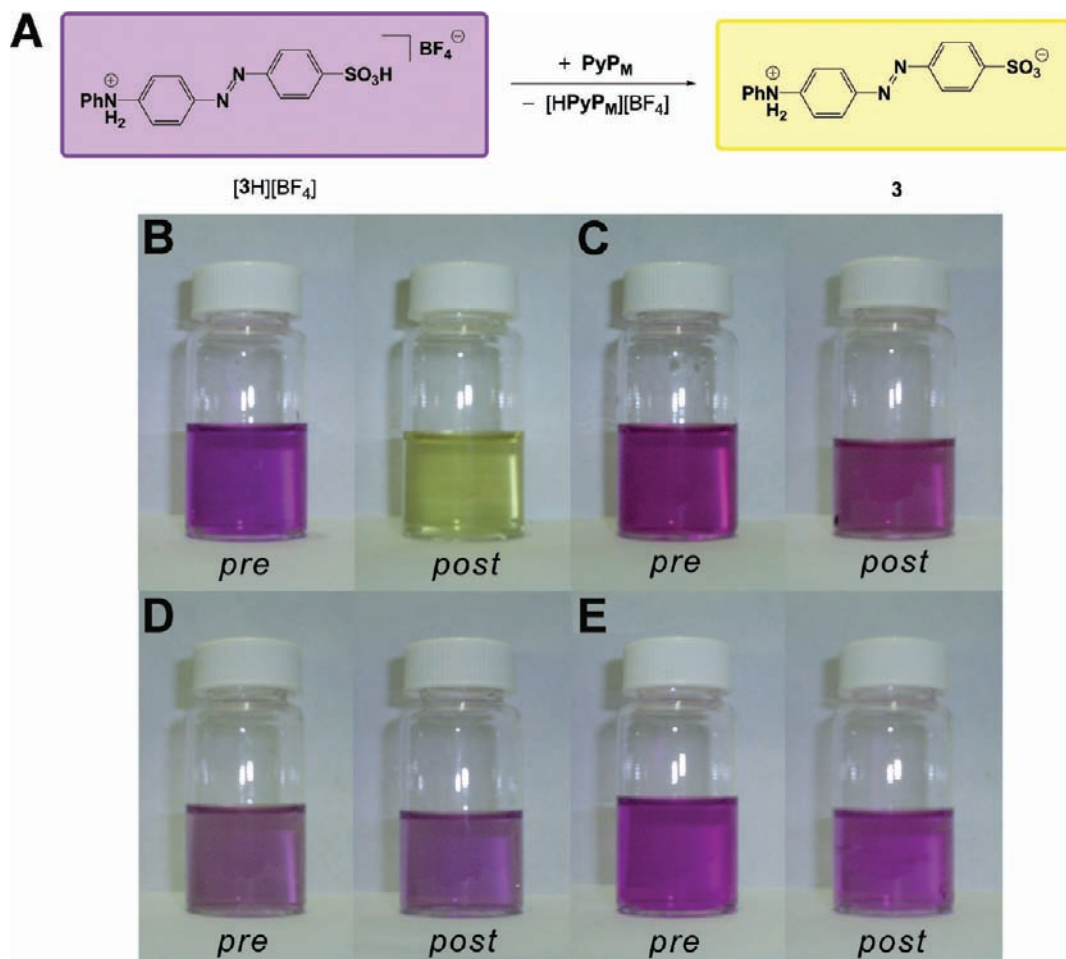
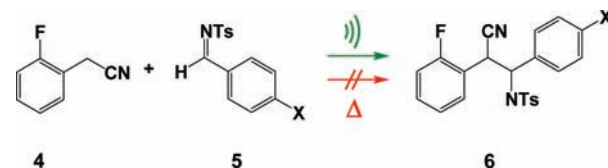


Figure 3. Strategy for and representative examples of colorimetric indicator experiments demonstrating generation of free PyP_M with corresponding negative control experiments. (A) Chemical reaction underlying the colorimetric response: the purple solution containing protonated dye $[3\text{H}][\text{BF}_4]$ was converted to a yellow solution containing **3** via deprotonation by PyP_M generated upon sonication. (B–E) Results of selected colorimetric indicator experiments and associated control experiments for $[(1)(\text{PyP}_M)_2]$. The solution containing $[(1)(\text{PyP}_{66})_2]$ changed from purple before sonication (pre) to yellow afterward (post) (B), indicating release of free PyP_{66} . No color change was observed during any of the negative control experiments (C–E). Conditions: sonication was performed for 2 h at 4 °C on a 10 mL CH_3CN solution containing 1 equiv of $[3\text{H}][\text{BF}_4]$ with respect to 10 μM analyte: (B) $[(1)(\text{PyP}_{66})_2]$, (C) $[(1)(\text{PyP}_{11})_2]$, (D) $[(2)(\text{PyP}_{110})_2]$, (E) $[(1)(\text{PyPiv})_2]$.

formation between allyl²⁰ or benzy²¹ cyanides and *N*-tosyl imines at ambient or lower temperatures. Moreover, van Koten has shown that these SCS-cyclopalladated complexes can be affixed to mesoporous silica and still exhibit their C–C bond forming catalytic function, suggesting that tethering a polymer chain could also preserve this activity.²² Because $[(1)(\text{PyP}_M)(\text{CH}_3\text{CN})]$ features a Pd center structurally homologous to that in $[(2)(\text{CH}_3\text{CN})]$, we reasoned that its generation via sonication of $[(1)(\text{PyP}_M)_2]$ would enable comparable catalytic function.

To test this hypothesis, a CH_3CN solution containing 2-fluorobenzyl cyanide (**4**), *N*-tosylbenzylimine (**5a**), and $[(1)(\text{PyP}_{66})_2]$ was subjected to the aforementioned sonication conditions (Scheme 1). After 2 h, an aliquot was removed and subsequently analyzed by gas chromatography (GC) which revealed 93%

Scheme 1. Palladium-Catalyzed Carbon–Carbon Bond Formation



conversion (70% isolated yield) to the known²¹ coupled product **6a** (Table 2). Performing this reaction with a more electron-deficient imine (**5b**) resulted in 98% conversion to **6b**, which was subsequently isolated in 71% yield. Alternatively, incorporating an electron-donating group into the imine (**5c**) completely quenched its reactivity, and no conversion to **6c** was noted. Given that this reaction formally proceeds via nucleophilic attack of a benzylic carbanion on an imine, it was unsurprising that increasing the electron density at the latter lowers its reactivity.²¹ No formation of **6a** or **6b** was catalyzed by $[(1)(\text{PyP}_{66})_2]$ in the absence of sonication, consistent with negligible thermal contribution to the observed conversion.²³ Analogous to the indicator experiments described above, negative control experiments were performed on the sonochemically activated coupling reaction for **6b** with (i) sub-threshold

(20) Aydin, J.; Szabó, K. J. *Org. Lett.* **2008**, *10*, 2881.

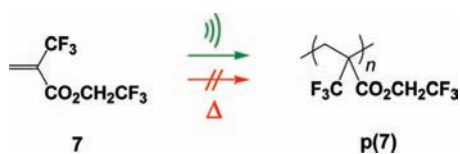
(21) Aydin, J.; Conrad, C. S.; Szabó, K. J. *Org. Lett.* **2008**, *10*, 5175.

(22) (a) Mehendale, N. C.; Sietsma, J. R. A.; de Jong, K. P.; van Walree, C. A.; Gebbink, R. J. M. K.; van Koten, G. *Adv. Synth. Catal.* **2007**, *349*, 2619. (b) Gagliardo, M.; Selander, N.; Mehendale, N. C.; van Koten, G.; Gebbink, R. J. M. K.; Szabo, K. J. *Chem.—Eur. J.* **2008**, *14*, 4800. (c) Kruithof, C. A.; Dijkstra, H. P.; Lutz, M.; Spek, A. L.; Gebbink, R. J. M. K.; van Koten, G. *Organometallics* **2008**, *27*, 4928.

Table 2. Selected Conversions and Yields for the Reactions Shown in Schemes 1 and 2^a

	5a → 6a ^{b,d} (X = H)	5b → 6b ^{b,d} (X = F)	7 → p(7) ^{c,e}
[(1)(PyP ₆₆) ₂]	93% (70%)	98% (71%)	42%
[(1)(PyP ₆₆) ₂] (no sonication)	3%	3%	—
[(1)(PyP ₇) ₂]	—	3%	—
[(2)(PyP ₁₁₀) ₂]	—	9%	—
[(1)(PyPiv) ₂] + 90 kDa PMA	—	3%	—

^a Unless specified otherwise, the sonication experiments were performed for 2 h at 4 °C. For **5** → **6** (a, X = H; b, X = F; c, X = NMe₂). Pd complex (i.e., [(1)(PyP₆₆)₂], [(1)(PyP₇)₂], [(2)(PyP₁₁₀)₂], or [(1)(PyPiv)₂] + 90 kDa PMA; 1.0 μmol) was combined with the following (either *b* or *c*, as indicated in table): ^b **4** (0.3 mmol, 1.5 equiv), **5** (0.2 mmol), Cs₂CO₃ (0.04 mmol, 20 mol %), and powdered 3 Å mol sieves (15 mg) in 10 mL of CH₃CN. ^c 3.0 mL of **7** (3.8 mmol) and 7 mL of CH₃CN. ^d Percent conversions were determined by GC using an internal standard (mesitylene); the numbers in parentheses correspond to isolated yields. For **5c** → **6c** (X = NMe₂), less than 3% conversion was observed under all conditions explored. ^e Percent yield determined relative to monomer consumption. See Tables S4 and S5, Supporting Information, for additional details.

Scheme 2. Pyridine-Catalyzed Anionic Polymerization

[(1)(PyP₇)₂], (ii) end-capped [(2)(PyP₁₁₀)₂], and (iii) mechanophore model [(1)(PyPiv)₂] in the presence of 90 kDa PMA. Because no formation of **6b** was observed in any of these control experiments, we conclude that the C–C coupling catalysis performed by [(1)(PyP₆₆)₂] was activated exclusively by mechanical force. The mechanical activation of such types of cross-coupling catalysts is envisioned to find utility in diagnostic and damage-reporting applications, where donor–acceptor conjugates with intense optical transitions may be formed in response to mechanical stress.^{5c}

Encouraged by the success with the carbon–carbon bond-forming reactions, we envisioned that the PyP_M released from [(1)(PyP_M)₂] during sonication may be similarly harnessed for base-mediated catalysis. Although pyridine-containing systems have been shown to catalyze a variety of polymerization reactions, these heteroaromatic species typically comprise electron-donating substituents that significantly enhance their nucleophilicities.²⁴ Drawn to a recent report by Willson who demonstrated²⁵ that pyridine is capable of initiating the anionic polymerization of α -trifluoromethyl-2,2,2-trifluoroethyl acrylate (**7**) at –78 °C in THF (Scheme 2), we envisioned that PyP_M, liberated upon sonication of [(1)(PyP_M)₂], may exhibit similar reactivity. Indeed, when a solution of [(1)(PyP₆₆)₂] and **7** in

CH₃CN was sonicated for 2 h, to ensure quantitative release of PyP₆₆, and then allowed to stir at 4 °C for 22 h to allow sufficient chain growth, the corresponding polymer **p(7)** (*M_n* = 23 kDa, PDI = 1.4; Table 2) was obtained in 42% yield with respect to monomer consumption.²⁶ No polymer was obtained in the absence of sonication under otherwise identical conditions, representing negligible thermal background formation of **p(7)**. Similarly, no polymerization occurred when a CH₃CN solution of **7** was sonicated with (i) sub-threshold [(1)(PyP₇)₂], (ii) end-capped [(2)(PyP₁₁₀)₂], or (iii) model complex [(1)(PyPiv)₂] in the presence of 90 kDa PMA. As observed for the Pd-catalyzed reactions, these results indicate that the anionic polymerization of **7** to **p(7)** was activated by mechanical force and proceeded via release of PyP₆₆ from [(1)(PyP₆₆)₂] during sonication. Initiation of comparable polymerization reactions in analogous mechanoresponsive materials could be harnessed to facilitate self-repairing functions in response to the formation or micro-cracks or other damage.^{6,8}

Conclusion

In summary, we have constructed a mechanoresponsive reagent, comprising a cyclometalated dipalladium-derived mechanophore and pyridine-capped PMA-based actuator, and demonstrated that chain scission occurs selectively at the metal–pyridine bond. This cleavage process produced catalytically active palladium and pyridine species with reactivities that could be harnessed to effect Pd-catalyzed C–C coupling and base-catalyzed anionic polymerization reactions, respectively. None of the aforementioned structural changes were observed (i) in the absence of sonication, or when (ii) the total mechanophore–actuator chain length was below the threshold required for the system to experience ultrasonication-induced mechanical force, (iii) the mechanophore was located at the end of the actuator chain, or (iv) the mechanophore was not covalently linked with an actuator. Collectively, our findings confirm that polymer chain scission occurred at the mechanophore–actuator bond and may be used to activate stoichiometric and catalytic reactions. The associated processes were unambiguously established to be mechanical in origin and may be used to access catalytic reaction pathways that are not attainable with the thermal energy supplied by the ambient reaction temperature. In a broader context, our results show that judicious selection of comparable mechanoresponsive reagents and methodologies could enable unknown chemical reactivities, as well as unprecedented advances in diagnostic, self-healing, and other types of stimulus-responsive materials.

Acknowledgment. We are grateful to the Army Research Office (grant No. W911NF-07-1-0409) and the Robert A. Welch Foundation (grant No. F-1621) for their generous financial support.

Supporting Information Available: Tables and figures summarizing control experiments and additional data. This material is available free of charge via the Internet at <http://pubs.acs.org>.

JA107620Y

- (23) We surmise that the catalytically active species sonochemically generated in solution from [(1)(PyP_M)₂] was [(1)(PyP_M)(CH₃CN)] in the presence of stoichiometric PyP_M, which would have different stereoelectronic properties and better organic solubility than those of synthetic precursors [(1)(CH₃CN)₂] or [(2)(CH₃CN)]. Indeed, [(1)(CH₃CN)₂] and [(2)(CH₃CN)] did not catalyze the coupling of **4** and **5** under strictly thermal conditions (0 °C, 0.5 mol% catalyst, 20 mol% Cs₂CO₃).
- (24) Kamber, N. E.; Joeng, W.; Waymouth, R. M.; Pratt, R. C.; Loheijer, B. G. G.; Hedrick, J. L. *Chem. Rev.* **2007**, *107*, 5813.
- (25) Strahan, J. R.; Adams, J. R.; Jen, W.; Vanleenhove, A.; Neikrik, C. C.; Rochelle, T.; Willson, C. G. *J. Micro/Nanolithog. MEMS MOEMS* **2009**, *8*, 043011.

- (26) Monomer consumption may have been curtailed by early termination processes due to the unoptimized polymerization reaction conditions employed. For example, **p7** (*M_n* = 30 kDa; PDI = 1.3) was obtained in 50% yield with respect to monomer consumption when PyP₆₆ was used as the pyridine source and similar conditions to the polymerization reaction performed under ultrasound described above were employed (see Table S5, Supporting Information).